Characteristic computed tomographic myelography findings in 23 Thoroughbred horses

Taro KONDO[1), Fumio SATO[2), Nao TSUZUKI[3), Kenichi WATANABE[3),
Noriyuki HORIUCHI[3), Yoshiyasu KOBAYASHI[3) and Kazutaka YAMADA[1)*

[1)School of Veterinary Medicine, Azabu University, Kanagawa, Japan
[2)Equine Research Institute, Japan Racing Association, Tochigi, Japan
[3)Department of Veterinary Medicine, Obihiro University of Agriculture and Veterinary Medicine, Hokkaido, Japan

ABSTRACT. The purpose of this observational study was to determine the characteristic computed tomographic (CT) myelography findings of cervical vertebral stenotic myelopathy (CVSM) lesions in Thoroughbred horses. A total of 23 Thoroughbred horses (age range, 155–717 days on CT examination; mean, 410.9 days) were analyzed. All 23 Thoroughbred horses underwent unenhanced radiography, radiographic myelography, and CT myelography. Unenhanced radiographs were observed the presence of cervical vertebral malalignment and osseous lesions. Radiographic myelograms were observed for signs of cervical spinal cord compression; additionally, CT myelograms were used to detect cervical vertebral osseous lesions. Ventral compressions were frequently observed in the cranial cervical vertebrae (C2–C4), whereas dorsal compressions were frequently observed in the caudal cervical vertebrae (C5–C7). Furthermore, osseous lesions of the caudal articular process developed more frequently than those of the cranial articular process. CT myelography in Thoroughbred horses is a useful method for detecting CVSM changes.

KEYWORDS: cervical vertebral stenotic myelopathy, computed tomography, myelography, radiography, Thoroughbred

Most horses born in Japan, around 80%, are Thoroughbred. Thus, Thoroughbred is the most important breed in Japanese equine industry. Cervical vertebral stenotic myelopathy (CVSM) is known as one of the orthopedic diseases in horses, especially Thoroughbred have a high prevalence [15]. And CVSM is a grave disease in Thoroughbred racehorse candidate and source of economic loss for owners. Two forms of CVSM have been described: type 1 is caused by vertebral malformation and/or malarticulation, which leads to dynamic instability and is most common among young horses, whereas type 2 is more often noted in older horses and results from cervical osteoarthritis, which leads to the static compression of the cervical spinal cord [11, 15].

Unenhanced radiographic examination is widely available in many veterinary clinics. Radiographic findings, including the subluxation and dorsal projection of the caudal epiphysis and osteophytes, suggest cervical abnormalities [13, 22]. A limitation of radiographic assessment is the use of intra- and intervertebral ratio, as this measurement has been reported to be unreliable with a variation of 5–10% [19]. Although, radiographic myelography may reveal the site and degree of dorsal and ventral compression, determining lateral compression remains challenging [20].

Equine computed tomography (CT), which was first introduced in 1987 [2], is widely used in equine veterinary clinics, and the examination of the cervical spinal cord in living horses has recently become feasible using this technique [17]. In case of showing neurological sign, CT myelography should be performed to evaluate the presence of spinal cord compression, or not. However, distinguishing between cervical spinal cord and cerebrospinal fluid via CT images is impossible as they have similar X-ray attenuation on CT. Therefore, contrast agent injection into the subarachnoid space is necessary to delineate the dura mater and pia mater. So far, CT myelography enables the most accurate diagnosis of CVSM in live horses [10, 14, 18, 21]. However, previous studies on CT myelography included various breeds of horses [10, 14, 21], not specific for Thoroughbred breed. Thus, we hypothesized that CVSM in Thoroughbred horses shows characteristic findings in CT myelography. In this observational study, we aimed to determine characteristic CT myelographic findings of CVSM in Thoroughbred horses.

*Correspondence to: Yamada, K.: kyamada@azabu-u.ac.jp, School of Veterinary Medicine, Azabu University, 1-17-71 Fuchinobe, Chuo-ku, Sagamihara, Kanagawa 252-5201, Japan

MATERIALS AND METHODS

Cases

Horses were admitted for gait abnormality involving lameness/neurological signs at rearing farms. A neurological examination was performed using the modified Mayhew's system, and a grading scale of 0–5 was used to classify the severity of clinical signs in the forelimbs and hindlimbs. Grade 0 indicated normal strength and coordination. Grade 1 indicated slight deficit on walking in tight circles. Grade 2 indicated mild spastic tetraparesis and ataxia at all times. Grade 3 indicated marked spastic tetraparesis and ataxia. Grade 4 indicated spontaneous stumbling, tripping, and falling. Grade 5 indicated recumbency, and unable to stand [7]. Primary veterinarians then carefully performed medical treatment. However, horses that were unfortunately not cured were referred to the Obihiro University of Agriculture and Veterinary Medicine for CT imaging to allow their owners to make a final decision on their potential as racehorses.

A total of 23 Thoroughbred horses (age range, 155–717 days on CT examination; mean, 410.9 days) were admitted to the Obihiro University of Agriculture and Veterinary Medicine between May 2016 and October 2019. The study population comprised 18 male horses (age range, 155–717 days on CT examination; mean, 398.6 days) and 5 female horses (age range, 201–628 days on CT examination; mean, 455.2 days). The study protocol was approved by the Animal Experiment and Welfare Committee of the Obihiro University of Agriculture and Veterinary Medicine (No. 27-127).

Unenhanced radiography

Unenhanced radiographies in standing horses were taken only lateral projection before myelography. All unenhanced radiography was performed by portable X-ray unit (PX-20BTmini, Kenko Tokina, Tokyo, Japan) and digital radiography (Aero DR, Konika-Minoluta, Tokyo, Japan). The imaging techniques were 90 kV, and 1.8–2.5 mAs.

Anesthesia

Horses underwent general anesthesia in both radiographic myelography and CT myelography. An indwelling intravascular catheter was placed into the jugular vein. All horses were premedicated intravenously with 5 µg/kg of medetomidine hydrochloride (Domitor, Nippon Zenyaku Kogyo, Tokyo, Japan), and anesthesia was induced using the intravenous administrations of 0.03 µg/kg of midazolam (Dormicum, Maruishi Pharmaceutical, Osaka, Japan) and 4 mg/kg of thiamylal (Isozol, Nichi-Iko Pharmaceutical, Toyama, Japan). Guaifenesin (25 mg/kg, Guaifenesin, Shinyo Pure Chemicals, Osaka, Japan) was rapidly infused until the horse became ataxic and conducted intratracheal intubation. Anesthesia was subsequently maintained using a triple drip mixture of guaifenesin (200 mg/kg/hr), xylazine (1 mg/kg/hr, Celactar, Bayer, Tokyo, Japan) and ketamine (2 mg/kg/hr, Ketalar, Daiichi-Sankyo, Tokyo, Japan).

Myelography

Radiographic myelography was examined performed at least one week before CT myelography. A 21-gauge spinal needle was inserted into the subarachnoid space via the atlanto-occipital junction under general anesthesia. Cerebrospinal fluid was allowed to drain out of the subarachnoid space for 2 min, after which the same volume of the contrast agent (300 mgI/ml, iohexol, Daiichi-Sankyo, Tokyo, Japan for radiographic myelography; 140 mgI/ml, iohexol, Teva Pharmaceutical Industries, Tokyo, Japan for CT myelography) as the drained cerebrospinal fluid was injected into the subarachnoid space. The horses' heads were lifted for 5 min, following which the horses underwent myelography.

Radiographic myelography were taken only lateral projection in lateral recumbency. All radiographic myelograms were obtained by portable X-ray unit (PX-20BTmini) and digital radiography (Aero DR). CT myelograms were obtained using a 16-row multidetector CT (Aquilion LB, Canon Medical Systems Corp., Ohtawara, Japan) with a gantry opening of 90 cm, tube voltage of 135 kV, tube current of 300 mA, and slice thickness of 0.5 mm. During CT examination, horses were placed in the dorsal position with the neck in a neutrally extended position on a large equine patient table.

Imaging evaluation

Unenhanced radiographs, radiographic myelograms, and CT myelograms were observed using digital imaging and communications in medicine viewer software (OsiriX-N, Newton Graphics, Sapporo, Japan). Additionally, sagittal and dorsal-plane images were fixed using Curved Multi Planar Reformation image-processing software (Virtual Place, Canon Medical Systems Corp.). All these images were read by K.Y., who is a Japanese Society of Equine Science certified veterinarian. Other three veterinarians (T.K., F.S., N.T.) were commented to initial diagnostic reports, and completed final diagnostic reports. Unenhanced radiographs were evaluated for the presence of cervical vertebral malalignment and osseous lesions. Compressions in radiographic myelography/CT myelography were defined a lack of the contrast agent due to an extradural mass effect with changes in the shape of the spinal cord [14]. CT myelograms additionally detected cervical vertebral osseous lesions.

Statistics

The distribution of cervical spinal cord compression was statistically analyzed (Excel add-in software, Multivariate, BellCurve for Excel, Tokyo, Japan). The ratio of cervical spinal cord compression of each intervertebral space site was calculated. The ratio of cervical spinal cord compression of each intervertebral space site was defined objective variable. And the place of cervical spinal compression was defined explanatory variable. Then, the objective variable and explanatory variable were analyzed by

regression analysis. The distribution of cervical vertebral osseous lesion was statistically analyzed. The ratio of cervical vertebral osseous lesion of each cervical vertebra was calculated. The ratio of cervical vertebral osseous lesion of each cervical vertebra was defined objective variable. And the place of cervical vertebra was defined explanatory variable. Then, the objective variable and explanatory variable were analyzed by regression analysis. Significance was defined as a P value of <0.05.

The stenotic ratio was calculated as the area of cervical spinal cord divided by that of the subarachnoid space in the transverse plane [25]. Cervical spinal cord stenotic ratio in each case was measured in six intervertebral space sites. Thus, a total of 138 cervical spinal cord sites (23 cases × 6 intervertebral space sites) were measured. The relationship between the modified Mayhew's system [7] and the stenotic ratio of the cervical spinal cord in the transverse plane, in which the largest cervical spinal cord stenotic ratio was selected in each case, was determined. A relationship between the degrees of cervical cord stenosis and ataxia was analyzed using regression analysis. Significance was defined as a P value of <0.05. The statistical analysis was performed using the Microsoft Excel.

Pathological examination

All cases were judged to have poor prognosis based on the clinical signs and CT myelograms as racehorse candidates. The decision to euthanize was made based on the potential of being a racehorse or not. The final decisions were made by the owners. The horses were euthanized using an excess dose of thiamylal sodium, following which they underwent necropsy. The cervical spinal cord was collected, fixed in 15% neutral-buffered formalin, cut into transverse sections, embedded in paraffin, and cut into 5-μm-thick sections. The paraffin-embedded sections were stained with hematoxylin and eosin for histopathological analysis. A total of 138 cervical spinal cord sites (23 cases × 6 intervertebral space sites) were evaluated by veterinary pathologists. The pathological findings, which were associated with Wallerian degeneration and subsequent demyelination; axonal swelling, myelin-laden macrophages, and myelin ovoid, were evaluated according to a previous textbook [7].

RESULTS

Unenhanced radiography

Seven horses had malalignment of the cervical vertebrae. Fourteen horses had cervical vertebral abnormalities involving osteophytes. By comparison, two horses did not show any cervical vertebral abnormalities (Fig. 1A and Table 1).

Radiographic myelography

Nineteen horses showed cervical spinal cord compression. In comparison, four horses were unplaceable cervical spinal cord compression sites (Fig. 1B and Table 1).
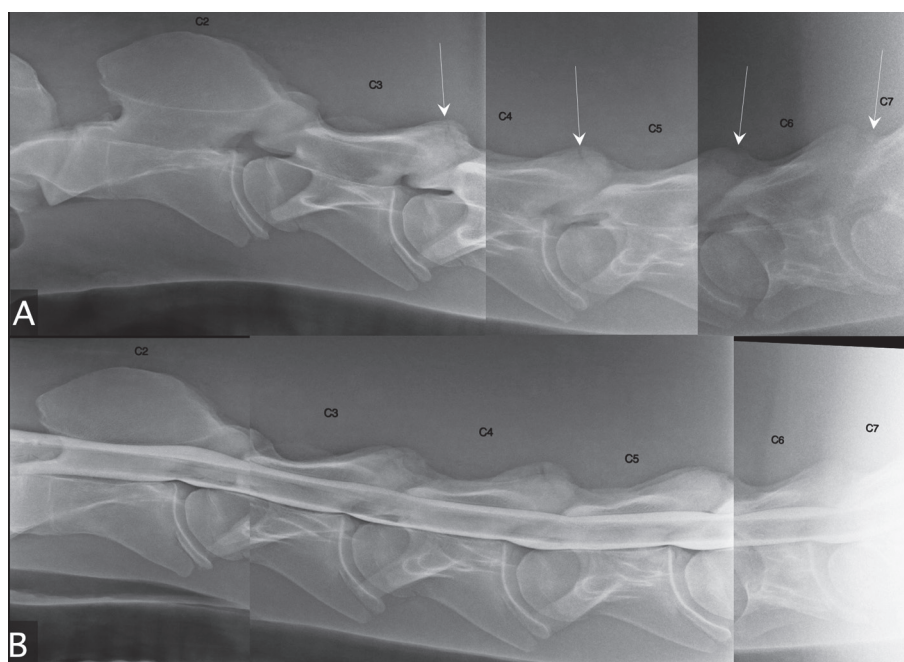

Fig. 1. Unenhanced radiograph (**A**) and radiographic myelogram (**B**) of case 23. The osseous lesions in C3, C4, C5 and C6 were observed by unenhanced radiograph (arrows), while cervical spinal cord compression was not observed by radiographic myelogram.

CT myelography

The CT images of the entire equine cervical vertebral column (C1–C7) were obtained in all 23 live horses. Cervical spinal cord compression was observed in 20 out of the 23 horses, with a total of 28 intervertebral space sites. The ventral compression of the cervical spinal cord was observed in 13 horses, with 17 intervertebral space sites. The dorsal compression of the cervical spinal cord was observed in 11 horses, with 11 intervertebral space sites (Fig. 2). The ventral compression of the cervical spinal cord was most frequently observed at C3–C4 (n=10), followed by C2–C3 (n=4). The dorsal compression of the cervical spinal cord was

Table 1. Case records, image findings, and pathological findings

	Sex	Age (days)	Weight (kg)	Meyhew system	Unenhanced radiograph	Radiographic myelography	CT myelography	Histopathological examination	
					Findings	Compression sites	Compression sites	Spinal cord lesion sites	Histopathological findings
Case1	Male	436	420	4	C5, C6, C7: osseous lesion	C5–C6	C2–C3, C5–C6	C2–C3, C3–C4, C5–C6	Wallerian degeneration
Case2	Male	258	330	1	C3–C4: malalignment	C3–C4	C3–C4	C4–C5	Wallerian degeneration
Case3	Male	374	450	1	C3–C4: malalignment	C3–C4–C5–C6	C3–C4, C4–C5	C5–C6, C6–C7	Wallerian degeneration
Case4	Male	414	438	0	Unplaceable	Unplaceable	Unplaceable	C1–C2	Leg bone cyst, Wallerian degeneration
Case5	Male	385	498	1	C5, C6: osseous lesion	C3–C4	Unplaceable	Unplaceable	Leg bone cyst
Case6	Male	175	245	0	Unplaceable	C3–C4–C5–C6	C4–C5, C5–C6	Unplaceable	Leg bone cyst
Case7	Female	201	297	0	C5, C6: osseous lesion	Unplaceable	C3–C4	Unplaceable	Non-purulent encephalitis, trigeminal neuritis, Hematoma
Case8	Male	454	435	2	C3–C4, C6–C7: malalignment	C3–C4, C5–C6–C7	C3–C4	C5–C6	Wallerian degeneration
Case9	Female	506	411	2	C6, C7: osseous lesion	C6–C7	C3–C4	C6–C7	Wallerian degeneration, axonal swelling, myelin-laden macrophages
Case10	Female	541	437	4	C6, C7: osseous lesion	C6–C7	C3–C4	C6–C7	Wallerian degeneration, axonal swelling, myelin-laden macrophages
Case11	Male	598	495	3	C5, C6: osseous lesion	C6–C7	C6–C7	C6–C7	Wallerian degeneration
Case12	Male	160	240	3	C3–C4: malalignment	C3–C4–C5	C2–C3, C3–C4	C3–C4	Wallerian degeneration, axonal swelling, myelin-laden macrophages
Case13	Male	155	270	3	C3–C4: malalignment	C3–C4–C5–C6–C7	C3–C4	C3–C4	Wallerian degeneration
Case14	Male	421	470	4	C5, C6: osseous lesion	C5–C6	C5–C6	C5–C6	Wallerian degeneration
Case15	Male	381	467	2	C3–C4: malalignment	C3–C4	C2–C3	C3–C4	Wallerian degeneration
Case16	Male	338	400	3	C3, C4: osseous lesion	C3–C4	C2–C3, C3–C4	C3–C4	Wallerian degeneration, demyelination, vacuolar degeneration
Case17	Male	426	426	3	C5, C6, C7: osseous lesion	C6–C7	C6–C7	C6–C7	Wallerian degeneration, demyelination, myelin-laden macrophages
Case18	Male	415	518	4	C5, C6: osseous lesion	Unplaceable	C5–C6	C5–C6	Wallerian degeneration, demyelination, myelin-laden macrophages
Case19	Male	717	488	2	C4, C5, C6: osseous lesion	C5–C6	Unplaceable	C2–C3, C5–C6	Wallerian degeneration
Case20	Female	628	472	3	C5, C6: osseous lesion	C5–C6	C2–C3, C5–C6	C4–C5, C6–C7	Wallerian degeneration, demyelination, myelin-laden macrophages
Case21	Male	388	393	1	C6, C7: osseous lesion	C6–C7	C4–C5, C5–C6	C1–C2, C2–C3, C3–C4, C4–C5, C6–C7	Wallerian degeneration, demyelination, myelin-laden macrophages
Case22	Male	680	523	3	C3–C4: malalignment	C3–C4	C3–C4, C5–C6	C5–C6	Wallerian degeneration, demyelination, myelin-laden macrophages
Case23	Female	400	205	5	C3, C4, C5, C6: osseous lesion	Unplaceable	C3–C4	C3–C4, C5–C6	Wallerian degeneration, demyelination, myelin-laden macrophages

C: Cervical vertebrae. A neurological examination was performed using the modified Mayhew's system, and a grading scale of 0–5 was used to classify the severity of clinical signs in the forelimbs and hindlimbs. Grade 0 indicated normal strength and coordination. Grade 1 indicated slight deficit on walking in tight circles. Grade 2 indicated mild spastic tetraparesis and ataxia at all times. Grade 3 indicated marked spastic tetraparesis and ataxia. Grade 4 indicated spontaneous stumbling, tripping, and falling. Grade 5 indicated recumbency, and unable to stand.

most frequently observed at C5–C6 (n=6), followed by C6–C7 (n=2). Ventral compressions were frequently observed in the cranial cervical vertebrae (C2–C4), whereas dorsal compressions were frequently observed in the caudal cervical vertebrae (C5–C7) (R^2=0.85, P<0.05). The median age (in days) on the CT examination of the cranial cervical spinal cord (C2–C4) compression was 393.7 days (range,155–680 days). The median age (in days) on the CT examination of the caudal cervical spinal cord (C5–C7) compression was 454.0 days (range,175–680 days).

The CT myelograms of the cervical vertebral osseous lesions are shown in Fig. 3. Cervical vertebral osseous lesions were observed in 20 out of the 23 horses, with a total of 56 sites. The right cranial articular processes with osseous lesions were observed in 9 horses, with 10 sites. The left cranial articular processes with osseous lesions were observed in 6 horses, with 6 sites. The right caudal articular processes with osseous lesions were observed in 12 horses, with 22 sites. The left caudal articular processes with osseous lesions were observed in 13 horses, with 18 sites (Fig. 4). Osseous lesions of the caudal articular process developed more frequently than those of the cranial articular process. (R^2=0.71, P<0.05). In total, there were 32 sites of the right articular process and 24 sits of the left articular process. The median age (in days) on the CT examination of the cervical vertebral osseous lesion, which was observed to be cranial to C4, was 361.7 days (range,155–717 days). The median age (in days) on the CT examination of the cervical vertebral osseous lesion, which was observed to be caudal to C5, was 429.4 days (range,155–717 days). Sixteen horses showed cervical vertebral osseous lesions at more than one site. Thirteen horses showed cervical vertebral osseous lesions on the same side of the cervical vertebrae.

The findings of hematoma and gas spot in the cervical vertebrae (Fig. 5) were observed in one horse each.
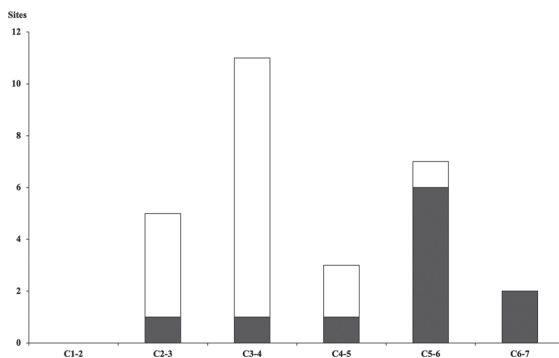

Fig. 2. Distribution of cervical spinal cord compression. Ventral compressions were most commonly observed in the cranial cervical spinal cord (n=17, white box show ventral compression). In comparison, dorsal compressions were most commonly observed in the caudal cervical spinal cord (n=11, gray box show ventral compression).

Relationship between the modified Mayhew's system and stenotic ratio

No significant differences between the modified Mayhew's system and stenotic ratio were observed (R^2=0.14, P=0.08) (Fig. 6).

Pathological examination

Among the 23 Thoroughbred horses, 20 exhibited histopathological lesions in the cervical spinal cord. The site of cervical spinal cord compression detected in CT myelograms and the site of histopathological change corresponded only in 11 horses.

Two horses, classified as Grade 0 using the modified Mayhew's system, had pathological bone cysts in their legs. One horse showed nonpurulent encephalitis and trigeminal neuritis (Table 1).

DISCUSSION

Previous studies on CT myelography included various breeds of horses [10, 14, 21]. This study focused on detecting characteristic changes in CT images of Thoroughbred horses less than 2 years of age that were racehorse candidates. Unenhanced radiographic examination findings have been considered important clues for
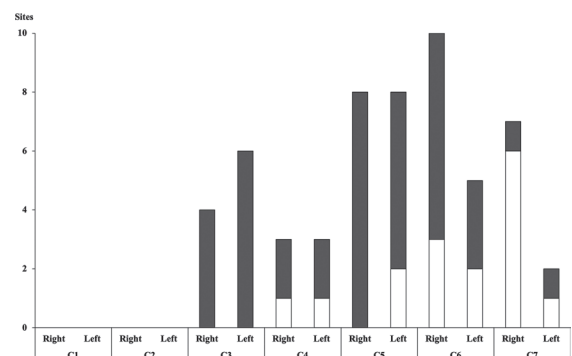

Fig. 3. CT myelograms (bone window; left: transverse plane, right: dorsal plane) of case 23. Both sides of the caudal articular process with osseous lesions in C3 were observed (arrows). Dorsal compressions of C3–C4, which were not observed by radiographic myelography, were observed by CT myelography.

Fig. 4. Distribution of cervical vertebral osseous lesions. The osseous lesions of the caudal articular process (n=40, gray box show caudal articular process) were occurred more frequently than those of the cranial articular process (n=16, white box show cranial articular process), whereas the osseous lesions of the cranial articular process were occurred more frequently than those of caudal articular process in C7.
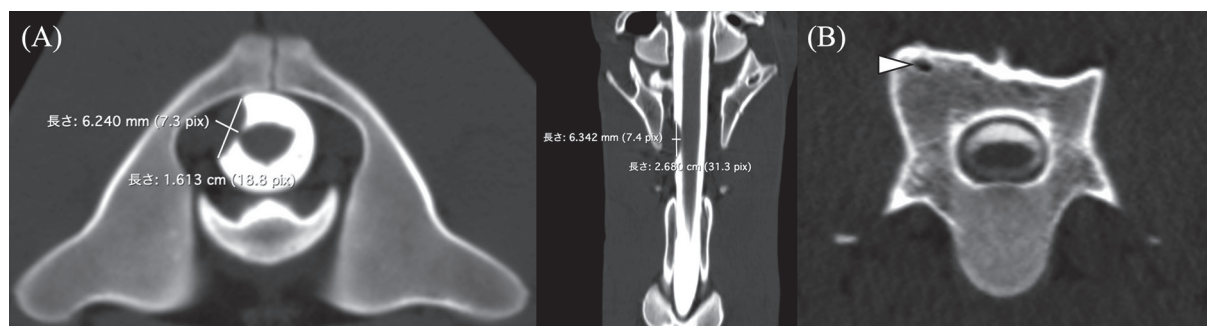
Fig. 5. CT myelograms (bone window). (**A**) Hematoma (6.2 mm × 16.1 mm, in transverse plane) in case 7 was observed in C1–C2. (**B**) A gas spot in case 22 was observed in C7 (arrowhead).
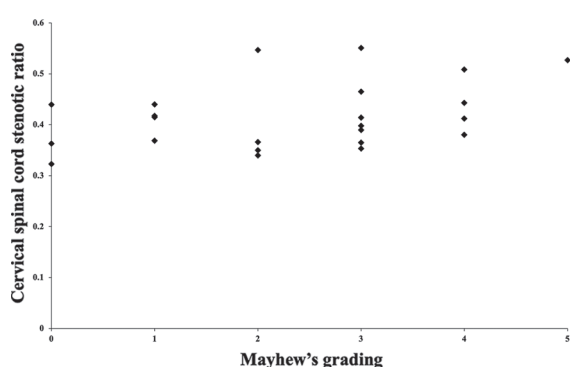

Fig. 6. Relationship between the modified Mayhew's system and cervical spinal cord stenotic ratio. No significant differences were observed between the modified Mayhew's system and cervical spinal cord stenotic ratio (N=23, R^2=0.14, P=0.08).

detecting cervical vertebral malalignment and osseous lesions [13, 22, 24]. However, unenhanced radiography cannot identify cervical spinal cord compression given the similar X-ray attenuation of the cervical spinal cord and cerebrospinal fluid. Therefore, myelography, wherein a contrast agent is injected into the subarachnoid space, has been utilized to determine cervical spinal cord compression [1, 12, 16, 22]. Moreover, recently, few studies reported that the radiographic changes of the articular process joint in radiography might not be of clinical significance [4, 5, 8]. In addition, the radiographic images of the cranial and caudal articular processes were indistinguishable. However, CT images were distinguishable between cranial and caudal articular processes.

Ventral compressions (type 1), with the median age (in days) of 393.7 days, were observed in cranial cervical vertebrae (C2–C4). The area of cranial cervical vertebrae (C2–C4) had inadequate strength ligaments [9], particularly in Thoroughbred young horses [6]. Rapid growth increases the risk of developmental orthopedic diseases, including CVSM [25]. Horse cervical vertebrae were lined up in an S-shaped arrangement, with load deflection points on C3–C4. In the view of the principle of leverage, the point of C3–C4 serves as the fulcrum point, and the head serves as the application point. The movement of head affects dorsoventral stress in C3–C4 owing to the up-and-down sequence of motion during galloping. Moreover, cranial cervical vertebral joint cannot be resistant to this moment. Meanwhile, the caudal cervical vertebral joint had adequate strength, even in young Thoroughbred horses [6]. Therefore, malalignment was less likely to occur in the caudal cervical vertebrae than in the cranial cervical vertebrae.

Dorsal compressions (type 2), with the median age (in days) of 454.0 days, were observed in caudal cervical vertebrae (C5–C7). The osseous lesions of the caudal articular process were developed more frequently than those of the cranial articular process. The caudal articular process is located dorsal side the cranial articular process. Thus, the caudal articular process might be easily affected by external impact involving fall and/or fight more easily.

Interestingly, in C7, the cranial articular processes were more affected than the caudal articular processes. This is our speculation that C6–C7 was affected by dorsoventral (vertical) stress at a low position while grazing [6]. The cranial articular processes were located under the caudal articular processes. Having a heavy neck with head and centripetal movement exerted a chronically heavy load to the part between C6 and C7, which especially affected the cranial articular processes of C7. Thus, C7 cranial articular process osseous lesions developed easily because of the principle of leverage. Previous studies on equine CT myelography have never described the articular processes separately as cranial and caudal [10, 14, 21]. This is the first report that evaluated the distribution of articular process osseous lesions.

In case 7, a hematoma was observed on CT myelography. The hematoma, which was confirmed by pathological examination, was a result of iatrogenic bleeding resulting from previous radiographic myelography. In case 22, a gas spot was observed on CT myelography. The cause of the gas spot remains unknown.

In our study, the 20 cervical spinal cord compression sites were observed in CT myelograms, and only 11 out of 20 horses shows histopathological change sites. This is supported by previous report so that pathological changes of the cervical spinal cord are not always consistent with cervical spinal cord compression on CT [14]. Even more the degrees of neurological score were not consistent with CT findings in this study. These conditions occurred owing to the following reason; neck position did not affect vertebral canal stenosis in healthy horses [3], but many horses with CVSM were easily affected by neck position due to cervical vertebral instability. In this study, horses were placed in the dorsal position with the neck in a neutrally extended position on an

equine patient table for CT. Therefore, cervical spinal cord compression when the horse neck was placed in the extension or flex position was not evaluated. It is open to discussion that flex position appeared to increase the detection of cervical spinal cord compression in the mid-cervical region but also substantially increased the frequency of false-positive diagnoses [14, 23]. Cervical spinal cord compression affecting horses with CVSM should be evaluated in each neck position. Moreover, cervical spinal cord compression in the standing position was not assessed using CT myelography because the horses were under general anesthesia in this study. In the future, the assessment of cervical spinal cord compression in the standing position is warranted.

A previous study described intervertebral disc mineralization [10], but it was not observed in the present study. This is because this study was performed in only Thoroughbred horses younger than 2 years of age. Accordingly, intervertebral disc mineralization might occur in specific species. Further, the Thoroughbred horses in this study were racehorse candidates, and their owners wanted to perform imaging diagnoses in the early stage when their horses were clinically suspected to have CVSM. As a result, CT examination in this study was performed before the occurrence of intervertebral disc mineralization due to cervical vertebral stress.

In conclusion, ventral compressions were observed in the cranial cervical vertebrae, whereas dorsal compressions occurred in the caudal cervical vertebrae. Furthermore, osseous lesions of the caudal articular process were occurred more frequently than those of the cranial articular process. These were the characteristic CT myelography findings of CVSM in Thoroughbred horses. CT myelography in Thoroughbred horses is a useful method for detecting CVSM changes.

REFERENCES

1. Aleman, M., Dimock, A. N., Wisner, E. R., Prutton, J. W. and Madigan, J. E. 2014. Atlanto-axial approach for cervical myelography in a Thoroughbred horse with complete fusion of the atlanto-occipital bones. *Can. Vet. J.* **55**: 1069–1073. [Medline]
2. Barbee, D. D., Allen, J. R. and Gavin, P. R. 1987. Computed tomography in horses. *Vet. Radiol. Ultrasound* **28**: 144–151. [CrossRef]
3. Beccati, F., Santinelli, I., Nannarone, S. and Pepe, M. 2018. Influence of neck position on commonly performed radiographic measurements of the cervical vertebral region in horses. *Am. J. Vet. Res.* **79**: 1044–1049. [Medline] [CrossRef]
4. Bergmann, W., de Mik-van Mourik, M., Veraa, S., van den Broek, J., Wijnberg, I. D., Back, W. and Gröne, A. 2020. Cervical articular process joint osteochondrosis in Warmblood foals. *Equine Vet. J.* **52**: 664–669. [Medline] [CrossRef]
5. Claridge, H. A. H., Piercy, R. J., Parry, A. and Weller, R. 2010. The 3D anatomy of the cervical articular process joints in the horse and their topographical relationship to the spinal cord. *Equine Vet. J.* **42**: 726–731. [Medline] [CrossRef]
6. Clayton, H. M. and Townsend, H. G. 1989. Cervical spinal kinematics: a comparison between foals and adult horses. *Equine Vet. J.* **21**: 193–195. [Medline] [CrossRef]
7. de Lahunta, A., Glass, E. and Kent, M. 2015. Large animal spinal cord disease. pp. 304–337. In: Veterinary Neuroanatomy and Clinical Neurology, 4th ed. (de Lahunta A, Glass E, Kent M, eds.), Elsevier Saunders, Philadelphia.
8. Espinosa-Mur, P., Phillips, K. L., Galuppo, L. D., DeRouen, A., Benoit, P., Anderson, E., Shaw, K., Puchalski, S., Peters, D., Kass, P. H. and Spriet, M. 2021. Radiological prevalence of osteoarthritis of the cervical region in 104 performing Warmblood jumpers. *Equine Vet. J.* **53**: 972–978. [Medline] [CrossRef]
9. Gellman, K. S. and Bertram, J. E. A. 2002. The equine nuchal ligament 1: structural and material properties. *Vet. Comp. Orthop. Traumatol.* **15**: 1–6. [CrossRef]
10. Gough, S. L., Anderson, J. D. C. and Dixon, J. J. 2020. Computed tomographic cervical myelography in horses: Technique and findings in 51 clinical cases. *J. Vet. Intern. Med.* **34**: 2142–2151. [Medline] [CrossRef]
11. Hahn, C. N., Handel, I., Green, S. L., Bronsvoort, M. B. and Mayhew, I. G. 2008. Assessment of the utility of using intra- and intervertebral minimum sagittal diameter ratios in the diagnosis of cervical vertebral malformation in horses. *Vet. Radiol. Ultrasound* **49**: 1–6. [Medline] [CrossRef]
12. Hudson, N. P. H. and Mayhew, I. G. 2005. Radiographic and myelographic assessment of the equine cervical vertebral column and spinal cord. *Equine Vet. Educ.* **17**: 34–38. [CrossRef]
13. Levine, J. M., Ngheim, P. P., Levine, G. J. and Cohen, N. D. 2008. Associations of sex, breed, and age with cervical vertebral compressive myelopathy in horses: 811 cases (1974–2007). *J. Am. Vet. Med. Assoc.* **233**: 1453–1458. [Medline] [CrossRef]
14. Lindgren, C. M., Wright, L., Kristoffersen, M. and Puchalski, S. M. 2021. Computed tomography and myelography of the equine cervical spine: 180 cases (2013–2018). *Equine Vet. Educ.* **33**: 475–483. [CrossRef]
15. Oswald, J., Love, S., Parkin, T. D. and Hughes, K. J. 2010. Prevalence of cervical vertebral stenotic myelopathy in a population of thoroughbred horses. *Vet. Rec.* **166**: 82–83. [Medline] [CrossRef]
16. Rose, P. L., Abutarbush, S. M. and Duckett, W. 2007. Standing myelography in the horse using a nonionic contrast agent. *Vet. Radiol. Ultrasound* **48**: 535–538. [Medline] [CrossRef]
17. Rovel, T., Zimmerman, M., Duchateau, L., Delesalle, C., Adriaensen, E., Mariën, T., Saunders, J. H. and Vanderperren, K. 2021. Computed tomographic examination of the articular process joints of the cervical spine in warmblood horses: 86 cases (2015–2017). *J. Am. Vet. Med. Assoc.* **259**: 1178–1187. [Medline] [CrossRef]
18. Rovel, T., Zimmerman, M., Duchateau, L., Adriaensen, E., Mariën, T., Saunders, J. H. and Vanderperren, K. 2021. Computed tomographic myelography for assessment of the cervical spinal cord in ataxic warmblood horses: 26 cases (2015–2017). *J. Am. Vet. Med. Assoc.* **259**: 1188–1195. [Medline] [CrossRef]
19. Scrivani, P. V., Levine, J. M., Holmes, N. L., Furr, M., Divers, T. J. and Cohen, N. D. 2011. Observer agreement study of cervical-vertebral ratios in horses. *Equine Vet. J.* **43**: 399–403. [Medline] [CrossRef]
20. Szklarz, M., Lipinska, A., Slowikowska, M., Niedzwiedz, A., Marycz, K. and Janeczek, M. 2019. Comparison of the clinical and radiographic appearance of the cervical vertebrae with histological and anatomical findings in an eight-month old warmblood stallion suffering from cervical

vertebral stenotic myelopathy (CVSM). *BMC Vet. Res.* **15**: 296–303. [Medline] [CrossRef]

21. Tucker, R., Hall, Y. S., Hughes, T. K. and Parker, R. A. 2022. Osteochondral fragmentation of the cervical articular process joints; prevalence in horses undergoing CT for investigation of cervical dysfunction. *Equine Vet. J.* **54**: 106–113. [Medline] [CrossRef]

22. van Biervliet, J., Mayhew, J. and de Lahunta, A. 2006. Cervical vertebral compressive myelopathy: diagnosis. *Clin. Tech. Equine Pract.* **25**: 54–59. [CrossRef]

23. van Biervliet, J., Scrivani, P. V., Divers, T. J., Erb, H. N., de Lahunta, A. and Nixon, A. 2004. Evaluation of decision criteria for detection of spinal cord compression based on cervical myelography in horses: 38 cases (1981–2001). *Equine Vet. J.* **36**: 14–20. [Medline] [CrossRef]

24. Withers, J. M., Voûte, L. C., Hammond, G. and Lischer, C. J. 2009. Radiographic anatomy of the articular process joints of the caudal cervical vertebrae in the horse on lateral and oblique projections. *Equine Vet. J.* **41**: 895–902. [Medline] [CrossRef]

25. Yamada, K., Sato, F., Hada, T., Horiuchi, N., Ikeda, H., Nishihara, K., Sasaki, N., Kobayashi, Y. and Nambo, Y. 2016. Quantitative evaluation of cervical cord compression by computed tomographic myelography in Thoroughbred foals. *J. Equine Sci.* **27**: 143–148. [Medline] [CrossRef]